Nanoscience and
Nanotechnology Letters
Vol. 9, 316–321, 2017

# Tailoring Structure and Magnetic Characteristics in $L1_0$-FePt Nanoparticles via Ag Doping in Different Valence States

Y. H. Jiang[1,2], Y. Liu[1,2,*], Y. X. Wang[1,2], L. Chen[1,2], X. L. Zhang[1,2], H. L. Liu[1,2], J. H. Yang[1,2,*], S. J. Li[3], D. D. Wang[4,*], and B. Yao[5]

[1] *Physics College of Jilin Normal University, Jilin Province 136000, People's Republic of China*
[2] *Key Laboratory of Functional Materials Physics and Chemistry (Jilin Normal University), Ministry of Education, Siping 136000, China*
[3] *Changchun Institute of Optics, Fine Mechanics and Physics, Chinese Academy of Sciences, Changchun 130033, China*
[4] *Technology Development Department, GLOBALFOUNDRIES Pte. Ltd. 60 Woodlands Industrial Park D, Street 2, 738406, Singapore*
[5] *Key Laboratory of Physics and Technology for Advanced Batteries (Ministry of Education), College of Physics, Jilin University, Changchun, 130012, China*

FePt, FePtAg and FePt–AgCl nanoparticles (NPs) are synthesized using the sol–gel method. The effect of Ag in different valence states on the morphology, chemical ordering and magnetic properties of $L1_0$-FePt NPs are studied in length. The addition of Ag to FePt NPs results in a larger particle size and wider distribution. Magnetic measurement results show that the coercivity (*Hc*) of FePt NPs is significantly higher with the addition of Ag in comparison with that of pure FePt NPs. While $Ag^+$ executes a negative impact on the magnetic performance of FePt NPs. The saturation magnetization (*Ms*) for the FePt, FePtAg and FePt–AgCl NPs are 15.6, 10.6 and 6.9 emu/g, respectively. The addition of non-magnetic Ag or AgCl to FePt dilutes the*Ms* value of the NPs. From X-ray diffraction analyses, we observe that the diffraction peaks become sharper and considerably increasing intensity when Ag or AgCl is added to the FePt sample.

**Keywords:** FePt Nanoparticles, Different Valence States, Structure, Magnetic Properties.

## 1. INTRODUCTION

Nanoparticles (NPs) have many of the usual physical and optical properties, including surface plasmon resonance, biosensing, energy conversion, gas sensing, data storage and catalyst.[1–14] As one of typical magnetic materials, $L1_0$ phase FePt NPs with face-centered tetragonal (FCT) structure are attractive as ultrahigh-density magnetic recording media due to their large magnetocrystalline anisotropy ($Ku \approx 10^7$ erg/cm$^3$) and good chemical stability.[15,16] Unfortunately, the as-synthesized FePt alloy possesses chemically disordered face-centered cubic (FCC) structure with a low coercivity, which is unsuitable for data storage.[17] High temperature (500 °C) annealing is necessary to covert the FCC structure to FCT structure.[18] The consequence of high temperature annealing is the breakdown of the surfactant coating, which causes the grain growth and the aggregation of the NPs.[19–21] The problems mentioned above are highly detrimental for maintaining ultra-high density bit cell sizes. In addition, high temperature annealing is a difficulty in controlling the direction of the magnetic easy axis; therefore, this will greatly limit their applications.

Many efforts have been made to reduce the annealing temperature required for phase transformation, using temperatures below where the particles aggregation, i.e., below the temperature where the organic surfactants decompose.[22–28] Doping engineering is widely used to tailor the band structures of bulk and nanoscale materials, promising and facilitating the construction of various multifunctional materials and devices.[29–37] Metals doping in FePt NPs were already proved to be effective ways to decrease the FCT ordering temperature.[38–42] As reported by Harrell et al. and Yu et al., the addition of a third metal such as Au or Ag has been found to be effective for lowering the ordering temperature in FePt NPs,[43,44] which is very interesting in terms of industrial scale production. However, in the method proposed by Harrell et al. the typically used of metal salt $Fe(CO)_5$ as a precursor was harmful and hazardous and a high temperature of 298 °C was still needed to prepare the as-synthesized FePt precursor

*Authors to whom correspondence should be addressed.


1941-4900/2017/9/316/006 doi:10.1166/nnl.2017.2306

before annealing. For these reasons, the proposed method is not suitable for industrial scale production.

In this report, FePt, FePtAg and FePt–AgCl NPs have been synthesized using the sol–gel method and we replaced $Fe(CO)_5$ with nontoxic $Fe(NO_3)_3 \cdot 9H_2O$. The role of the third metal along with its effect on the transformation kinetics has been studied. The differences in the magnetic properties of FePt, FePtAg and FePt–AgCl with respect to the heat-treatment temperatures were also studied. To the best of our knowledge, the study of the effect of Ag in different valence states on the magnetic properties of $L1_0$-FePt NPs is unprecedented.

## 2. EXPERIMENTAL DETAILS

The metal precursors used are $C_6H_8O_7 \cdot H_2O$, $H_2PtCl_6 \cdot 6H_2O$, $Fe(NO_3)_3 \cdot 9H_2O$, $AgNO_3$ and $NaBH_4$ in the appropriate quantities in order to synthesize $(FePt)_{75}(AgCl)_{25}$ and $(FePt)_{75}Ag_{25}$ samples, while the molar ratio of Fe/Pt was constantly kept equal to 3/2. The detailed synthetic procedure via the sol–gel method for FePt nanoparticles is described in our previous work.[45]

For $(FePt)_{75}(AgCl)_{25}$ sample, the key modification was adding a certain amount of $AgNO_3$ after obtaining the mixed solution of $Fe(NO_3)_3 \cdot 9H_2O$, $H_2PtCl_6 \cdot 6H_2O$ and $C_6H_8O_7 \cdot H_2O$. After stirring, the solution was polymerized to form a gel at 80 °C. With precursors heat-treated in argon gas for 2 h at 650 °C and with the heating rate of 10 °C $min^{-1}$, $(FePt)_{75}(AgCl)_{25}$ NPs were successfully synthesized. In a typical procedure for preparing $(FePt)_{75}Ag_{25}$ NPs, a certain amount of $Fe(NO_3)_3 \cdot 9H_2O$, $H_2PtCl_6 \cdot 6H_2O$ and $C_6H_8O_7 \cdot H_2O$ were firstly dissolved in the deionized water to form a sol. To avoid AgCl aggregate in the sample, $AgNO_3$ was dissolved in $NaBH_4$ to obtain metallic silver. Then the solution was washed with alcohol and deionized water for three times and separated by centrifugation. The appropriate amount of metallic silver was added to the sol. Finally, $(FePt)_{75}Ag_{25}$ NPs were successfully synthesized after the same post-annealing treatment as above described. Herein, we obtained the $(FePt)_{75}(AgCl)_{25}$ and $(FePt)_{75}Ag_{25}$ samples named as FePt–AgCl, FePtAg according to the elements may be contained in the samples. For comparison, we also prepared pure FePt sample in the similar process without any addition.

X-ray diffraction (XRD) patterns were recorded by a MAC Science MXP-18 X-ray diffractometer using a Cu target radiation source was used to study the crystal structure and morphology of the samples. The transmission electron microscope (FEI Tecnai F30 TEM) spectroscopy system was used to qualitatively confirm the detailed microscopic structure. X-ray photoelectron spectroscopy (XPS, VG ESCALAB Mark II) was used to assess the chemical state and surface composition of the deposits. The magnetic properties of the samples were measured by a Lake Shore 7407 vibrating sample magnetometer (VSM).

## 3. RESULTS AND DISCUSSION

XRD patterns of the FePtAg and FePt–AgCl NPs, after annealing at 650 °C under an Ar atmosphere, are shown in Figure 1(a). As a reference, the XRD pattern of pure FePt NPs annealed at the same temperature is also shown in Figure 1(a). All of the samples show the superlattice reflections (001) and (110) as well as clearly splitting of the (200)/(002) peak which signifies a tetragonality $L1_0$ FePt. Furthermore, compared with that of pure FePt sample, we observe that the diffraction peaks become sharper and considerably increasing intensity when Ag element added to the FePt sample. With the Ag addition, the peaks become sharper due to the increase particle size as well as the enhanced crystallinity. For the FePtAg sample, the peak at $2\theta = 38.13°$, 44.32° and 64.45° corresponds to Ag metal [JCPDS No. 04-0783], which is further demonstrated below by TEM and XPS studies. The enlarged XRD pattern of the FePt–AgCl sample is shown in Figure 1(b). Besides the diffraction peaks from the $L1_0$ FePt, the presence of diffraction peaks at $2\theta = 27.9°$, 32.3°, 46.3° and 57.6°, these correspond to the (111), (200), (220) and (222) planes for the cubic phase AgCl [JCPDS No. 31-1238]. And no diffraction peaks from the cubic Ag phase are observed.

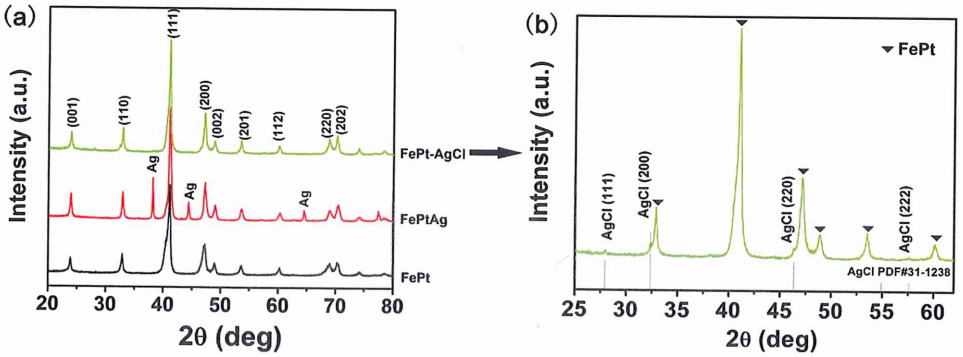


**Fig. 1.** XRD patterns of (a) FePt, FePtAg and FePt–AgCl NPs annealed for 650 °C and (b) enlarged view of FePt–AgCl sample.

The lattice constants are derived from MDI Jade 6.5 program. As for the FePt, FePtAg and FePt–AgCl samples, the lattice constants are estimated to be $a = b = 3.846 \pm 0.004$ Å, $c = 3.713 \pm 0.003$ Å, $a = b = 3.849 \pm 0.001$ Å, $c = 3.715 \pm 0.002$ Å and $a = b = 3.855 \pm 0.001$ Å, $c = 3.723 \pm 0.002$ Å, respectively. The average particle size is calculated by Scherrer equation using the full-width at half maximum of the FePt (111) peak from the XRD patterns.[46] Results show average grain size of FePt, FePtAg and FePt–AgCl NPs is 12.8, 23.4 and 27.7 nm, respectively. These indicate that additive Ag promotes the grain growth. This result is similar to previously reported findings.[47]

To demonstrate the transformation process quantitatively, a chemical order parameter $S$ is introduced. In general, quantitative values of $S$ are obtained from the comparison between the integrated intensities of the superlattice and fundamental reflections of XRD. An approximate relation between $S$ and $c/a$, which can be obtained and expressed as

$$S^2 = \frac{1-(c/a)}{1-(c/a)_{Sf}} \quad (1)$$

where $(c/a)_{Sf}$ is the $c/a$ value of the fully ordered FePt NPs;[48–50] $(c/a)$ is the value of the partially ordered FePt NPs. The $c$ and $a$ are the lattice constants of the FePt NPs with FCT structure. By Eq. (1), the $S$ value of the FePt, FePtAg and FePt–AgCl NPs samples are 0.89, 0.92 and 0.88, respectively. It is clearly observed that $S$ exhibits a maximum value at the FePtAg NPs.

Figure 2 shows the microstructure of FePt (Figs. 2(a, b)) and FePtAg NPs (Figs. 2(c, d)) by TEM. The FePt NPs without Ag additive are hexagonally arranged with a very uniform spherical shape, and an average particle size of about 12–13 nm (Fig. 2(a)). While as shown in Figure 2(c), the size of the FePtAg NPs range from 20 to 30 nm, and the particle sintering is apparent, which indicates that Ag additive resulted in a larger particle size and wider distribution for the NPs. Figure 2(b) shows the HRTEM image of a typical FePt NP. The lattice distance is 0.220 nm, approaching the ideal value of the (111) plane of the $L1_0$-FePt lattice. The inset in Figure 2(b) shows SAED patterns is composed of (001), (110), (111), (200), (220) and (311) diffraction rings, indicating that an FCT phase structured FePt crystal had been formed. This result is in

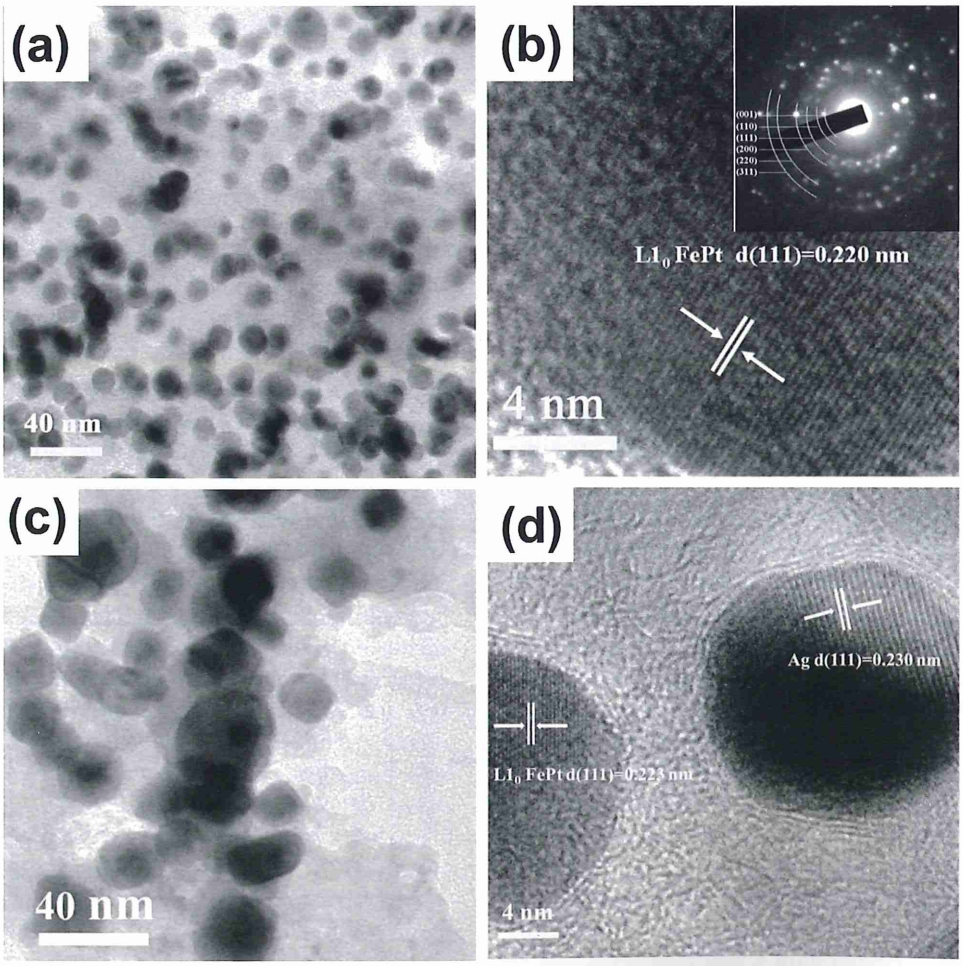


**Fig. 2.** (a) TEM image (b) HRTEM image with SAED pattern as an inset of FePt NPs and (c) TEM image and (d) HRTEM image of FePtAg NPs.

agreement with XRD data in Figure 1. Considering that the lattice distance of FCT FePt NPs differs from that of FCC silver (e.g., $d_{FCTFePt(111)} = 0.222$ nm and $d_{Ag(111)} = 0.235$ nm),[51,52] an significant difference of lattice fringe spacing between the FePt and Ag lattice could be distinguished through HRTEM. We conducted detailed HRTEM measurements on the FePtAg sample. The HRTEM images in Figure 2(d) show distinct planes with different *d*-spacing values. The distances 0.223 nm between the lattice fringes match closely to the $L1_0$ FePt plane (111), while the *d*-spacing 0.230 nm corresponds to (111) plane of silver.

XPS measurement was carried out to identify phase compositions and chemical states of Ag and Pt elements in the FePt, FePtAg and FePt–AgCl samples (Fig. 3). For the FePtAg NPs (Fig. 3(a)), the Ag 3*d* spectrum consists of two peaks at about 367.6 and about 373.7 eV, which correspond to the binding energies of Ag $3d_{5/2}$ and Ag $3d_{3/2}$, respectively, typical of metallic silver.[53] The result is in agreement with the XRD pattern. As shown in (Fig. 3(b), the peaks of Ag $3d_{5/2}$ and Ag $3d_{1/2}$ are detected at 367.1 and 373.1 eV for the FePt–AgCl sample, which corresponds to the peaks positions of $Ag^+$ state,[54] with a doublet separation of $\Delta = 6$ eV (Fig. 3(b)).[55] These XPS spectra above match well with literature data.[56] The XPS spectrum of Pt for the FePt sample shows double peaks with binding energies of 70.8 and 74.1 eV (Fig. 3(d)), which correspond to the standard peaks of pure Pt $4f_{7/2}$ and Pt $4f_{5/2}$.[57] For the FePtAg NPs, the positions of the Pt peaks are situated at 70.2 and 73.6 eV. As is seen from the above results, the positions of Pt $4f_{7/2}$ and Pt $4f_{5/2}$ peaks slightly shift towards the lower binding energy side, which might be caused by the alloying process of Fe and Pt.[58]

Figure 4 shows the hysteresis loops for FePt, FePtAg and FePt–AgCl NPs after annealing at temperatures of 650 °C. For the FePt NPs without Ag additive, the coercivity (*Hc*) shows a relatively large value and reaches about 7070 Oe, which may be attributed to the formation of the $L1_0$ FePt phase. There is an obvious increase in *Hc* for the FePt NPs after adding Ag atoms, where it has a coercivity value of around 9400 Oe. This is in contrast to the FePt NPs prepared in the absence of Ag. We deduce that the increase of the *Hc* is mainly determined by the increases of the ordering degree a chemical order parameter *S* and average grain size. It indicates that Ag addition is effective to enhance the ordering degree and promote the magnetic properties of FePt NPs. A small hysteresis loop about 2850 Oe was observed for the FePt–AgCl sample. We consider that excess AgCl produce a negative effect on the magnetic performance of the FePt NPs. In addition, the saturation magnetization (*Ms*) of FePt, FePtAg and FePt–AgCl are 15.6, 10.6 and 6.9 emu/g, respectively (Fig. 4). It can be

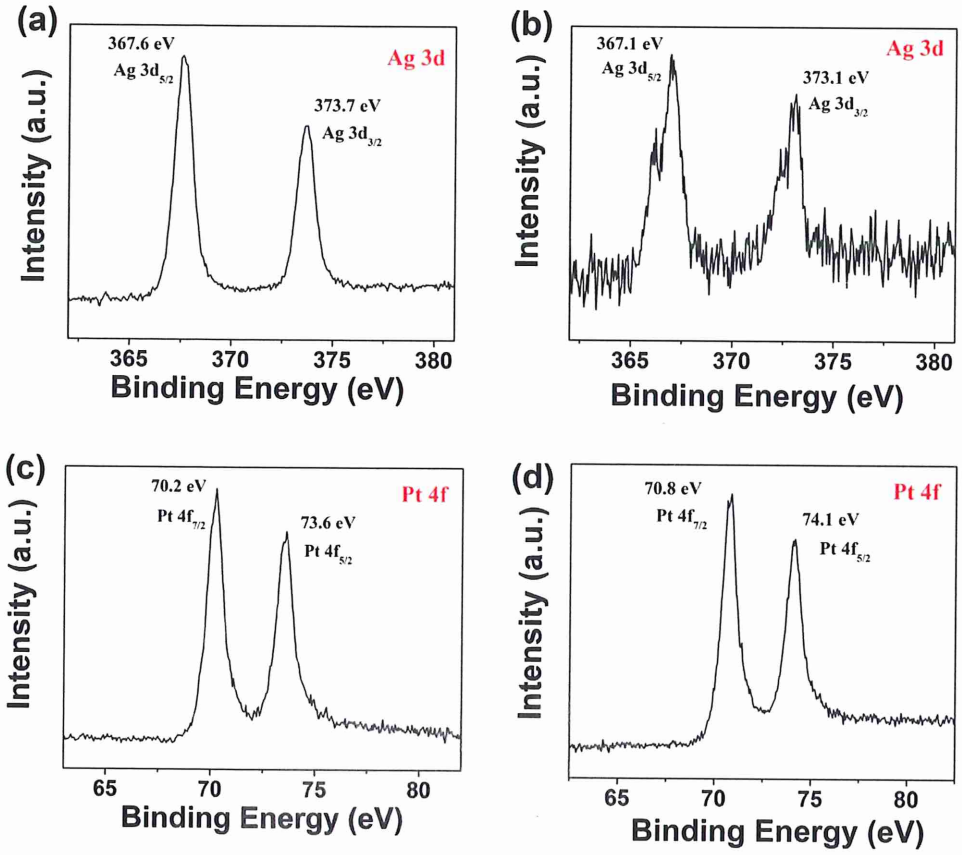


**Fig. 3.** High-resolution scans of the XPS spectra for (a, c) Ag 3*d*, Pt 4*f* for FePtAg NPs, (b) Ag 3*d* for FePt–AgCl NPs and (d) Pt 4*f* for FePt NPs.

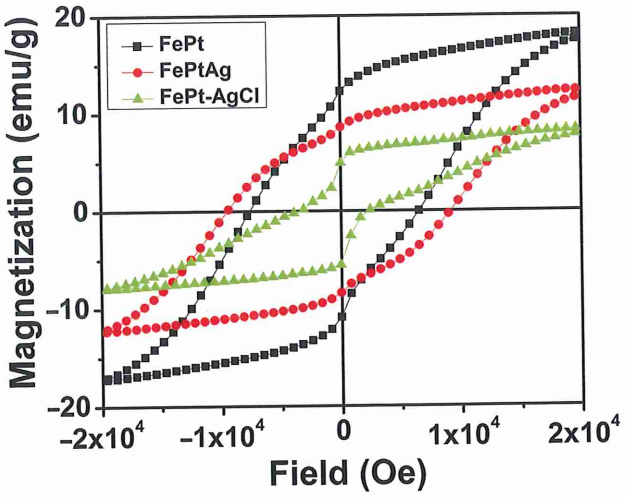


**Fig. 4.** Magnetic hysteresis ($M$–$H$) loops of FePt, FePtAg and FePt–AgCl NPs at room temperature under 20 kOe.

seen that the *Ms* reduces with the Ag or $Ag^+$ addition in FePt NPs. Since Ag and AgCl are non-magnetic, the addition of Ag or AgCl to FePt will dilute the *Ms* value of the NPs. The similar decline trend is also observed by You et al.[59]

## 4. CONCLUSIONS

In this work, FePt, FePtAg and FePt–AgCl NPs have been synthesized by the sol–gel method. Here the changes in the structural and magnetic properties of these NPs and the effect of adding silver in different valence states to FePt in comparison to pure FePt have been investigated. TEM observations reveal a narrow size distribution with particle diameter of about 12–13 nm for FePt NPs without Ag or $Ag^+$ additive. Whereas grain growth and particle sintering is observed for the FePtAg NPs. But silver additive showed positive effect on the chemical ordering and magnetic properties of the FePt NPs. The addition of $Ag^+$ to FePt alloy promotes grain growth, however, reduces the chemical ordering and magnetic properties compared to pure FePt. The parameters *Ms* reduces with the addition of Ag or AgCl to FePt NPs.

**Acknowledgments:** This work is supported by the National Natural Science Foundation of China (Grant Nos. 21546013 and 61575080), National Youth Program Foundation of China (Grant no. 51609100), Program for New Century Excellent Talents in University (NCET-13-0824 and NCET-11-0981), Program for the development of Science and Technology of Jilin province (Item Nos. 20160101287JC and 20150520015JH) and Program for the development of Science and Technology of Jiangsu province (Item No. BK20130477).

## References and Notes

1. Y. Kang, X. Ye, J. Chen, L. Qi, R. E. Diaz, V. Doan-Nguyen, G. Xing, C. R. Kagan, J. Li, R. J. Gorte, E. A. Stach, and C. B. Murray, *J. Am. Chem. Soc.* 135, 1499 (**2013**).
2. P. Wang, Y. P. Wang, and L. M. Tong, *Light: Sci. Appl.* 2, e102 (**2013**).
3. K. Ariga, J. Li, J. B. Fei, Q. M. Ji, and J. P. Hill, *Adv. Mater.* 28, 1251 (**2016**).
4. C. C. Lu, X. Y. Hu, K. B. Shi, Q. Hu, R. Zhu, H. Yang, and Q. H. Gong, *Light: Sci. Appl.* 4, e302 (**2015**).
5. J. C. Kim and E. J. Park, *Nanosci. Nanotechnol. Lett.* 7, 697 (**2015**).
6. P. K. Shrestha, Y. T. Chun, and D. Chu, *Light: Sci. Appl.* 4, e259 (**2015**).
7. R. Kuchi, K. Lee, Y. Lee, C. Luong, K. Lee, B. Park, and J. Jeong, *Nanosci. Nanotechnol. Lett.* 7, 734 (**2015**).
8. C. F. Guo, T. Sun, F. Cao, Q. Liu, and Z. Ren, *Light: Sci. Appl.* 3, e161 (**2014**).
9. H. Abe, J. Liu, and K. Ariga, *Mater. Today* 19, 12 (**2016**).
10. Y. H. Su, Y. F. Ke, S. L. Cai, and Q. Y. Yao, *Light: Sci. Appl.* 1, e14 (**2012**).
11. S. Lee, I. Cho, and Y. Sohn, *J. Nanosci. Nanotechnol.* 15, 8362 (**2015**).
12. J. Yang, F. Luo, T. S. Kao, X. Li, G. W. Ho, J. Teng, X. Luo, and M. Hong, *Light: Sci. Appl.* 3, e185 (**2014**).
13. L. L. Gao, S. F. Li, and T. F. Cao, *Chin. J. Liq. Crys. Disp.* 30, 925 (**2015**).
14. A. E. Cetin, A. F. Coskun, B. C. Galarreta, M. Huang, D. Herman, A. Ozcan, and H. Altug, *Light: Sci. Appl.* 3, e122 (**2014**).
15. J. Wang, H. S. Amin, Y. K. Takahashi, S. Okamoto, S. Kasai, J. Y. Kim, T. Schrefl, and K. Hono, *Acta Mater.* 111, 47 (**2016**).
16. Y. Liu, Q. W. Kou, S. Xing, C. Y. Mao, N. Kadasala, Q. Han, J. L. Song, H. L. Liu, Y. Q. Liu, Y. S. Yan, and J. H. Yang, *Nanosci. Nanotechnol. Lett.* 7, 665 (**2015**).
17. K. S. Rao, T. Balaji, Y. Lingappa, M. R. P. Reddy, A. Kumar, and T. L. Prakash, *Physica B* 405, 3205 (**2010**).
18. T. Iwamoto, Y. Kitamoto, and N. Toshima, *Physica B* 404, 2080 (**2009**).
19. S. Park, G.-J. Sun, H. Kheel, S. K. Hyun, and C. Lee, *Nanosci. Nanotechnol. Lett.* 7, 703 (**2015**).
20. J. He, B. Bian, Q. Zheng, J. Du, W. Xia, J. Zhang, A. Yan, and J. P. Liu, *Green Chem.* 18, 417 (**2016**).
21. M. Liu, P. Hu, G. Zhang, Y. Zeng, H. W. Yang, J. Fan, L. Jin, H. N. Liu, Y. Deng, S. Li, X. Zeng, S. Elingarami, and N. Y. He, *Theranostics* 4, 71 (**2015**).
22. C. L. Platt, K. W. Wierman, E. B. Svedberg, R. van de Veerdonk, J. K. Howard, A. G. Roy, and D. E. Laughlin, *J. Appl. Phys.* 92, 6104 (**2002**).
23. M. Almansour, L. Sajti, W. Melhim, and B. Jarrar, *Nanosci. Nanotechnol. Lett.* 7, 763 (**2015**).
24. J. H. Wang, Z. Ali, N. Y. Wang, W. B. Liang, H. N. Liu, F. Li, H. W. Yang, L. He, L. B. Nie, N. Y. He, and Z. Y. Li, *Sci. China Chem.* 58, 1774 (**2015**).
25. R. Kuchi, K. Lee, Y. Lee, C. Luong, K. Lee, B. Park, and J. Jeong, *Nanosci. Nanotechnol. Lett.* 7, 734 (**2015**).
26. S. Kang, J. W. Harrell, and D. E. Nikles, *Nano Lett.* 2, 1033 (**2002**).
27. S. H. Lee and S. H. Eun, *Physica B* 406, 2646 (**2011**).
28. S. Wang, S. S. Kang, D. E. Nikles, J. W. Harrell, and X. W. Wu, *J. Magn. Magn. Mater.* 266, 49 (**2003**).
29. G. H. Kim, L. Shao, K. Zhang, and K. P. Pipe, *Nat. Mater.* 12, 719 (**2013**).
30. G. Z. Xing, J. B. Yi, F. Yan, T. Wu, and S. Li, *Appl. Phys. Lett.* 104, 202411 (**2014**)
31. J. J. Lee, G. Z. Xing, J. B. Yi, T. Chen, M. Ionescu, and S. Li, *Appl. Phys. Lett.* 104, 012405 (**2014**).
32. D. D. Wang, G. Z. Xing, F. Yan, Y. S. Yan, and S. Li, *Appl. Phys. Lett.* 104, 022412 (**2014**).

**33.** D. D. Wang, Q. Chen, G. Z. Xing, J. B. Yi, S. R. Bakaul, J. Ding, J. L. Wang, and T. Wu, *Nano Letters* 12, 3994 (**2012**).
**34.** S. V. Sergeyev, C. B. Mou, E. G. Turitsyna, A. Rozhin, S. K. Turitsyn, and K. Blow, *Light: Sci. Appl.* 3, e131 (**2014**).
**35.** T. Grossmann, T. Wienhold, U. Bog, T. Beck, C. Friedmann, H. Kalt, and T. Mappes, *Light: Sci. Appl.* 2, e82 (**2013**).
**36.** E. M. Dianov, *Light: Sci. Appl.* 1, e12 (**2012**).
**37.** Z. J. Xi, R. R. Huang, Z. Y. Li, N. Y. He, T. Wang, E. B. Su, and Y. Deng, *ACS Appl. Mater. Interfaces* 7, 11215 (**2015**).
**38.** Y. Liu, Y. H. Jiang, N. Kadasala, X. L. Zhang, C. Y. Mao, Y. X. Wang, H. L Liu, X. N. Jiang, J. H. Yang, and Y. S. Yan, *J. Sol–Gel Sci. Techn.* 72, 156 (**2014**).
**39.** H. Y. Zhu, S. Zhang, S. J. Guo, D. Su, and S. H. Sun, *J. Am. Chem. Soc.* 135, 7130 (**2013**).
**40.** S. S. Kang, D. E. Nikles, and J. W. Harrell, *J. Appl. Phys.* 93, 7178 (**2003**).
**41.** Y. Liu, Y. H. Jiang, N. Kadasala, X. L. Zhang, C. Y. Mao, Y. X. Wang, H. L Liu, Y. Q. Liu, J. H. Yang, and Y. S. Yan, *J. Solid State Chem.* 215, 167 (**2014**)
**42.** L. Y. Lu, D. Wang, X. G. Xu, H. C. Wang, J. Miao, and J. Jiang, *Mater. Chem. Phys.* 129, 995 (**2011**).
**43.** J. W. Harrel, D. E. Nikles, S. S. Kang, X. C. Sun, Z. Jia, S. Shi, J. Lawson, G. B. Thompson, C. Srivastava, and N. V. Seetala, *Scripta Mater.* 53, 411 (**2005**).
**44.** Y. S. Yu, P. Mukherjee, Y. Tian, X.-Z. Li, J. E. Shield, and D. J. Sellmyer, *Nanoscale* 6, 12050 (**2014**).
**45.** J. H. Yang, Y. H. Jiang, Y. Liu, X. L. Zhang, Y. X. Wang, Y. J. Zhang, J. Wang, W. Li, and X. Cheng, *Mater. Lett.* 91, 348 (**2013**).
**46.** U. Holzwarth and N. Gibson, *Nanotechnol.* 6, 534 (**2011**).
**47.** H. B. Wang, P. Shang, J. Zhang, M. W. Guo, Y. P. Mu, Q. Li, and H. Wang, *Chem. Mater.* 25, 2450 (**2013**).
**48.** S. Hsiao, S. Chen, F. T. Yuan, H. W. Huang, Y. D. Yao, and H. Y. Lee, *J. Magn. Magn. Mater.* 310, e775 (**2007**).
**49.** Y. Endo, N. Kikuchi, O. Kitakami, and Y. Shimada, *J. Appl. Phys.* 89, 7065 (**2001**).
**50.** S. Mitani, K. Takanashi, H. Nakajima, K. Sate, R. Schreiber, P. Grünberg, and H. Fujimori, *J. Magn. Magn. Mater.* 156, 7 (**1996**).
**51.** J. Kim, C. Rong, Y. Lee, J. P. Liu, and S. Sun, *Chem. Mater.* 20, 7242 (**2008**).
**52.** T. Wen, D. X. Zhang, J. Liu, H. X. Zhang, and J. Zhang, *Chem. Commun.* 51, 1353 (**2015**).
**53.** Y. C. Her, Y. C. Lan, W. C. Hsu, and S. Y. Tsai, *Jpn. J. Appl. Phys.* 43, 267 (**2004**).
**54.** V. Andal and G. Buvaneswari, *Sensor Actuat. B-Chem.* 155, 653 (**2011**).
**55.** L. Kuai, B. Geng, X. Chen, Y. Zhao, and Y. Luo, *Langmuir* 26, 18723 (**2010**).
**56.** D. B. Ingram, P. Christopher, J. L. Bauer, and S. Linic, *ACS Catal.* 1, 1441 (**2011**).
**57.** G. Zhao, R. Mo, B. Wang, L. Zhang, and K. Sun, *Chem. Mater.* 26, 2551 (**2014**).
**58.** Y. S. Lee, K. Y. Lim, Y. D. Chung, C. N. Whang, and Y. Jeon, *Surf. Interface Anal.* 30, 475 (**2000**).
**59.** C. Y. You, Y. K. Takahashi, and K. Hono, *J. Appl. Phys.* 100, 056105 (**2006**).


Received: 2 July 2016. Accepted: 20 September 2016.